Reactive and Functional Polymers 209 (2025) 106186

Contents lists available at ScienceDirect

Reactive and Functional Polymers

journal homepage: www.elsevier.com/locate/react

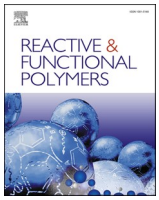

# High glass transition catalyst-free polybenzoxazine vitrimer through one-pot solventless method

Festus Ifeanyi Anagwu [a,*], Eleftheria Dossi [b], Alexandros A. Skordos [a]

[a] Composites and Advanced Materials Centre, School of Aerospace, Transport and Manufacturing, Cranfield University, Cranfield MK43 0AL, United Kingdom
[b] Centre for Defence Chemistry, Cranfield University, Defence Academy of United Kingdom, Shrivenham, Swindon SN6 8LA, UK

ARTICLE INFO

*Keywords:*
Polybenzoxazine
Vitrimer
Aerospace
Composites

ABSTRACT

A high glass transition polybenzoxazine has been synthesised by a one-pot solventless method via the Mannich condensation of a phenolic disulphide, paraformaldehyde and aniline. The solventless process reduces synthesis time, material costs, and the need for post-synthesis purification. The polybenzoxazine exhibits a glass transition temperature ($T_g$) of 155°C and thermosetting behaviour below this temperature. Dynamic disulphide bond metathesis associated with a topological freezing temperature of 78°C and an activation energy of 127 kJ mol$^{-1}$ delivers vitrimeric functionality with fast, catalyst-free stress relaxation above $T_g$. This material fully relaxes stress within 5 s at 190°C, with thermal degradation beginning above 250°C. It exhibits a glassy modulus of 3.6 GPa, high char yield (57.4%) translating to a high limiting oxygen index (*LOI*) of 40.5% and excellent environmental resistance, as evidenced by low water uptake (1.4%) after immersion at 75°C for 31 days. The combination of environmental resistance, due to thermosetting character, high glass transition, facile synthesis, high char yield, good processability, and fast stress relaxation position this polybenzoxazine as a promising candidate matrix system for repairable aerospace thermosetting continuous fibre composites.

## 1. Introduction

Vitrimers have attracted the attention of the polymer science community in the last decade due to their combination of thermosetting performance (environmental resistance and high mechanical strength) and thermoplastic reprocessability without compromising their integrity. Since their discovery [1], epoxy vitrimer systems are the most widely studied class [2–5], due to the current dominance of epoxy systems in the composites industry relative to other resins such as phenolics, benzoxazines, bismaleimides, and polyimides. There is currently a research focus on the design of polybenzoxazine vitrimers as alternatives to epoxies, also motivated by the advantages of polybenzoxazines compared to both epoxies and phenolics in terms of thermomechanical and hygrothermal performance, fire retardancy, low cure shrinkage, molecular design flexibility, dimensional stability, and compatibility with sustainable precursors.

Various vitrimer chemistries have been explored to synthesise benzoxazine vitrimers, including boronic ester bond [6] and transesterification exchange chemistry [7,8]. The synthesis of a healable benzoxazine crosslinked with boronic ester bond involves the use of toxic and flammable toluene as solvent in a time-consuming three-pot strategy that includes a purification step, whilst established benzoxazine vitrimers based on transesterification are synthesised via two distinct steps: esterification of a phenolic precursor using an acid, followed by synthesis of benzoxazine using the esterified phenolic. This strategy has been applied to synthesise systems involving the purification of the esterified precursor prior to use in benzoxazine synthesis [7–9], yielding moderate to high glass transition temperature ($T_g$) materials, with transesterification bond exchange catalysed by the benzoxazine tertiary amine [10]. Other reprocessable polybenzoxazines exhibiting dynamic covalent bond exchange do so through dioxaborolane metathesis [11] and transcarbamoylation [12], with low $T_g$ of 29°C and 55°C, respectively. The synthesis of these benzoxazines involves multiple steps. Whilst the former is synthesised by mixing a cardanol-based benzoxazine thermoset with 1,4-phenylenebisboronic acid and water at ambient temperature followed by treatment with magnesium sulphate, forming boronic bond in the monomer, the latter involves reacting hexamethylene diisocyanate with crude benzoxazine monomer made from tyrosol, dodecylamine, and paraformaldehyde in the presence of dibutyltin dilaurate catalyst, producing a hybrid polybenzoxazine-polyurethane vitrimer system. Similarly, self-healability of

* Corresponding author.
*E-mail addresses:* f.i.anagwu@cranfield.ac.uk (F.I. Anagwu), e.dossi@cranfield.ac.uk (E. Dossi), a.a.skordos@cranfield.ac.uk (A.A. Skordos).

https://doi.org/10.1016/j.reactfunctpolym.2025.106186
Received 17 November 2024; Received in revised form 11 January 2025; Accepted 31 January 2025
Available online 1 February 2025

polybenzoxazine main chain is achieved by mixing benzoxazine with phenyl boronic acid in chloroform prior to curing; this has been successfully applied in synthesising a low temperature self-healing benzoxazine system [13].

A polybenzoxazine obtained by the polymerisation of a two-component mixture of main-chain benzoxazine and polyether amine exhibits characteristic stress-relaxation, dynamic bond exchange between primary and secondary amines, and reprocessability with moderate $T_g$ (97–108°C) and topology freezing temperatures in the range of 39–97°C [14], depending on polyether amine content, whilst a set of imine bond-enabled polybenzoxazine vitrimers with $T_g$ in the range of 34–160°C [15] are synthesised via a solventless approach that involves multiple steps, more complex than traditional benzoxazine synthesis pathways [16]. A high-temperature benzoxazine vitrimer has been formulated from a main-chain benzoxazine and an epoxide-functionalised polyrotaxane, yielding an interlocked network and a covalent adaptable network with improved ductility and toughness, with tin(II) 2-ethylhexanoate-catalysed transacetalation [17].

Disulphide metathesis is an effective bond exchange for catalyst-free vitrimers [18]. Systems incorporating disulphide bonds feature a fast evolution of stress relaxation at moderate temperature (100–140°C) and have been achieved with benzoxazine using a simple implementation of one-pot solventless Mannich condensation reaction [19,20], resulting in a vitrimer appropriate for low temperature applications due to a $T_g$ of 40°C.

The current study was motivated by the need to develop high temperature catalyst-free benzoxazine vitrimers ($T_g \geq 143$°C, excellent char yield and low water uptake for wet environment applicability) for aeronautics applications, following the cost-effective one-pot solventless method [16]. The hypothesis in this work is that this is achievable if the phenolic and amine precursors are endowed with molecular structural functionalities that could translate into moderate-to-high crosslinking density upon polymerisation of the new benzoxazine monomer, and there is a high degree of aromaticity in the polymer to guarantee high char yield and potential hydrophobicity. In addition to this, the precursors must exhibit a high level of mutual solubility at typical benzoxazine synthesis temperatures (80–130°C) without solidifying prior to oxazine ring formation. Combined with disulphide chemistry, this can deliver a benzoxazine system featuring high glass transition and fast catalyst-free stress relaxation leading to vitrimeric functionality.

In this work, the vitrimeric property of a high-$T_g$ benzoxazine monomer bearing disulphide bond is reported. The monomer – previously synthesised by Endo et al. through the reaction of 4,4′-dihydroxydiphenyl disulphide (DHPDS), 1,3,5-triphenyl-1,3,5-triazine, a cyclocondensate of aniline and formaldehyde using toluene as solvent – was used as a precursor for highly polymerizable benzoxazine bearing thioether moiety [21–23]. The current work uses a solventless process to synthesise the same molecule, reducing synthesis time, cost of materials and the need for post-synthesis purification. The solventlessly synthesised benzoxazine monomer was chemically characterised using nuclear magnetic resonance (NMR) and Fourier transform infrared (FTIR) spectroscopy, whilst the thermal properties of both monomer and polymer were investigated by differential scanning calorimetry (DSC). The degradation behaviour of the polymer was investigated by thermogravimetric analysis (TGA), whilst the van Krevelen approximation for limiting oxygen index (*LOI*) [24] was used to assess the prospects of the material as a potential flame retardant. Furthermore, swelling experiments were performed to establish the thermosetting character of the polymer. Dynamic mechanical analysis (DMA) was used to measure the glassy modulus and $T_g$, whereas stress relaxation was used to estimate the vitrimer topological freezing temperature. Scratching and healing experiments – quantified through profilometry of surface profiles before and after healing a scratched specimen – were utilised to demonstrate the self-healing functionality of the vitrimer as a matrix system for repairable aerospace thermosetting continuous fibre composites.

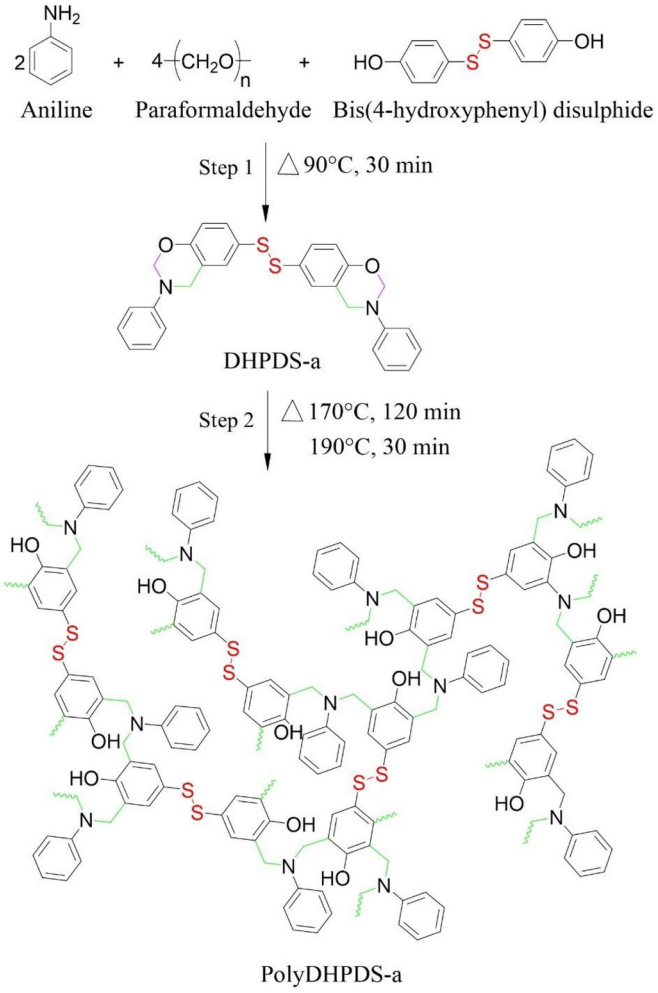


**Scheme 1.** Synthesis (Step 1) and polymerisation (Step 2) of DHPDS-a[1]. Red: disulphide moiety; Green: oxazine ring Phe-$CH_2$-N linkage. Purple; oxazine ring O-$CH_2$-N linkage.

## 2. Materials and methods

### 2.1. Materials

Bis(4-hydroxyphenyl) disulphide (CAS number: 15015573; 98%) was purchased from AmBeed USA [25]. Aniline (CAS number: 62533;

99.8%) was purchased from Fisher Scientific [26], and paraformaldehyde (CAS number: 30525894) was purchased from Sigma Aldrich/Merck [27]. All chemicals were used as received without any further treatment.

### 2.2. Synthesis and polymerisation of 1,2-bis(3-phenyl-3,4-dihydro-2H-benzo[e][1,3]oxazin-6-yl)disulphane (DHPDS-a)

The benzoxazine monomer, 1,2-bis(3-phenyl-3,4-dihydro-2H-benzo[e][1,3]oxazin-6-yl) disulphane (DHPDS-a), was synthesised using stoichiometric amounts of aniline, paraformaldehyde and bis(4-hydroxyphenyl) disulphide (2:4:1 mol ratio) following a one-pot solventless method [28]. Paraformaldehyde (2.40 g, 80 mmol) was added to aniline (3.72 g, 40 mmol) and the mixture kept under magnetic stirring for 10 min at room temperature. Bis(4-hydroxyphenyl) disulphide (5 g, 20 mmol) was added at room temperature and the reaction mixture was then heated at 90°C under stirring (300 rpm) for 30 min. A brown viscous DHPDS-a monomer (92 % yield) was obtained. The synthesis and polymerisation are shown in steps 1 and 2 of Scheme 1.

To cast plates of polyDHPDS-a, the monomer (solid at room temperature) was placed on a glass plate, bounded by silicone rubber and gradually heated to 80°C on a hot plate, allowing the viscous liquid to homogeneously spread on the glass plate up to the boundary formed by the silicone rubber frame. A second glass plate was used to form the casting cavity. The resin was degassed at 110°C for 10 min, after which the vacuum was turned off and the assembly was then clamped and placed into an OV301 precision curing vacuum oven (Easy composites). The temperature of the oven was ramped to the cure temperature (170°C) at a heating rate of 4°C $min^{-1}$. The resin was cured at 170°C for 2 h and post-cured at 190°C for 30 min, to ensure full polymerisation and attainment of the polymer ultimate glass transition temperature.

### 2.3. Characterisation

#### 2.3.1. NMR measurements

The chemical structure of soluble samples (typically 20 mg $mL^{-1}$) was analysed by proton and carbon nuclear magnetic resonance ($^{1}H$ NMR and $^{13}C$ NMR, respectively) spectroscopy in deuterated dimethyl sulfoxide (DMSO-$d_6$, Goss Scientific, >99.9%), at ambient temperature using a Bruker Ascend 400 MHz spectrometer with a double resonance broadband BBFO probe and tetramethylsilane (TMS, Goss Scientific, >99.5%) as an internal reference.

#### 2.3.2. Fourier transform infrared (FTIR) spectroscopy

FTIR spectroscopic data were acquired in transmission mode with a SMART iTR Nocolet iZ10 spectrometer (Thermo Fisher Scientific) from 600 to 4000 $cm^{-1}$. One hundred background and sample scans were performed with a resolution of 4.0 $cm^{-1}$, sample gain of 8.0, optical velocity of 0.4747 cm $s^{-1}$ and aperture of 80.0 mm.

#### 2.3.3. Differential scanning calorimetry (DSC)

The cure behaviour of DHPDS-a was studied by DSC, using a DSC 250 Discovery (TA Instruments) equipped with an RCS cooling system under nitrogen purge at 50 mL $min^{-1}$. Experiments were conducted by encapsulating resin in a Tzero aluminium pan and scanning at 10°C $min^{-1}$ from −50°C to 240°C to measure the uncured material glass transition, exothermic cure onset temperature, cure peak temperature and heat of reaction. The cured sample was rescanned at 10°C $min^{-1}$ to measure the cured polymer $T_g$.

#### 2.3.4. Thermogravimetric analysis (TGA)

TGA was performed on a Discovery TGA 550 (TA Instruments) under nitrogen (60 mL $min^{-1}$) at 10°C $min^{-1}$ heating rate from 50°C to 910°C. Samples were placed in a 100 μL platinum pan. The Limiting Oxygen Index (*LOI*) of the polymer, which can be used as an indication of flame retardancy, was approximated according to the van Krevelen empirical relation[24]:

$$LOI = 17.5 + 0.4CR_{850} \quad (1)$$

where $CR_{850}$ is the char yield in weight % at 850°C.

#### 2.3.5. Dynamic mechanical analysis (DMA) and stress relaxation

DMA and stress relaxation experiments were carried out on a Q800 DMA (TA Instruments) in tension mode using a single cantilever setup (2-point bending). The dimensions of specimens were 35 ± 0.5 mm × 8 ± 0.2 mm × 2 ± 0.05 mm. Dynamic DMA tests with a heating rate of 3°C $min^{-1}$ in the 30–250°C range, frequency of 1 Hz, and amplitude of 15 μm were performed to measure the storage and loss moduli as functions of temperature and identify the $T_g$. The crosslinking density of the polymer was determined using the relation:

$$d = \frac{E'}{3RT} \quad (2)$$

where $d$ is the crosslinking density, $E'$ is the rubbery storage modulus of the polymer measured with DMA, $R$ is the universal gas constant, and $T$ is absolute temperature. Stress relaxation experiments were conducted at five isothermal temperatures of 175, 180, 185, 190, and 195°C. The specimens were preloaded with a force of 1 mN and subsequently deformed to an applied strain of 2% after equilibration to the desired isothermal temperature. The decay of relaxation modulus with time was recorded, and the relaxation time was estimated as the time required for the modulus to drop from its plateau value by 1/e.

#### 2.3.6. Rheology

Rheological measurements were carried out on an AR2000ex rheometer (TA Instruments) equipped with a water cooling system using a 2° cone and plate configuration with 40 mm cone diameter and truncation depth of 54 μm. The gap setting in the rheometer was equal to the truncation of the cone. The viscosity evolution of the monomer was monitored in dynamic flow mode using shear rate of 300 $s^{-1}$ at 2°C $min^{-1}$ ramp rate from 70°C to 153°C.

#### 2.3.7. Swelling tests

Swelling experiments were performed using deionised (DI) water, ethanol, acetone, dimethyl formamide (DMF), dimethyl sulfoxide (DMSO) at room temperature (22 ± 2°C) and hot DI water at 75°C. In these tests, polyDHPDS-a samples of about 50 mg were immersed in 10 mL of solvent for 31 days (744 h). The samples were removed at 5, 24, 72, 240, 408, 567 and 744 h, surface-cleaned with tissue paper and weighed to obtain the swelling ratio ($W$) using:

$$W = \frac{m_s}{m_i} - 1 \quad (3)$$

where $m_i$ and $m_s$ are the initial and swollen sample masses, respectively. After each measurement, the sample was returned to the solution as fast as possible. The samples were removed after 31 days, dried in an oven at 50°C for 24 h and weighed to obtain the dry mass after swelling. The soluble fraction ($M$) was calculated using:

$$M = 1 - \frac{m_d}{m_i} \quad (4)$$

where $m_d$ is the mass of the sample after drying. To ensure statistical reliability of the swelling data, 4 samples of the polymer were used for each solvent and average results used for data analysis.

#### 2.3.8. Healing

The healability of polyDHPDS-a was demonstrated through recovery of a scratch manually made on a cured specimen using a T5016 heavy duty single edge razor blade (Agar Scientific). The profile of the scratch was measured using a Bruker Dektak XT profilometer with a stylus range

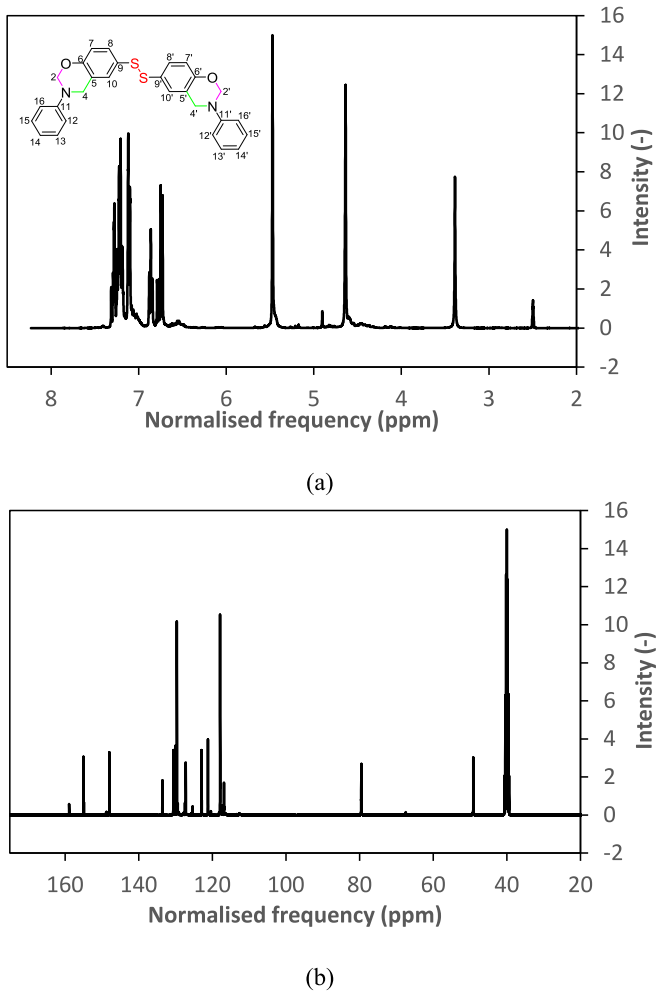


**Fig. 1.** NMR spectra of DHPDS-a in DMSO-$d_6$. (a) $^{1}$H NMR. (b) $^{13}$C NMR.

of 524 μm, scan length of 1500 μm and scan resolution of 0.25 μm. The specimen was subsequently clamped between two flat pieces of aluminium and placed in the oven at 190°C for 15 min, followed by cooling down. The depth of the scratch after healing was measured with the profilometer and compared with the results obtained before healing.

The dataset underlying this study and its description can be accessed through the Figshare repository at https://doi.org/10.6084/m9.figshare.26196461 [29].

## 3. Results and discussion

### 3.1. Synthesis of DHPDS-a

The $^{1}$H NMR spectrum of DHPDS-a monomer recorded in DMSO-$d_6$, was characterised by two sets of multiplet signals: (i) between 7.43 ppm and 7.10 ppm assigned to twelve aromatic protons attached to 10, 12–16 and 10′, 12′-16′ carbon atoms and (ii) between 6.90 ppm and 6.70 ppm attributed to four aromatic protons attached to carbon atoms in 7, 8 and 7′, 8′ positions as shown in Fig. 1(a). Additionally, two singlet signals at 5.47 ppm and 4.63 ppm were assigned to the absorptions of eight protons attached to carbon atoms in 2, 4 and 2′, 4′ positions for a total of 24 protons in DHPDS-a molecule. The two small broad peaks centred at 6.60 ppm and 7.20 ppm were attributed to impurities due to formation of oligomeric species of benzoxazine, resulting from the potentially pre-opened oxazine rings during synthesis. The signal at 3.35 ppm and 2.50 ppm were assigned to protons from water in DMSO-$d_6$ and DMSO-$d_6$ solvent, respectively. The DHPDS-a monomer was used in the next step

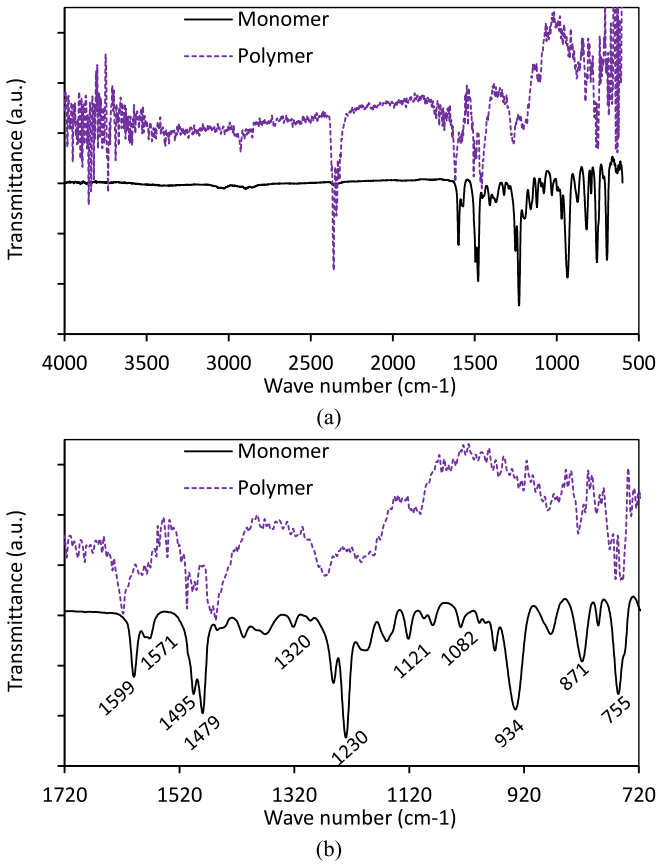


**Fig. 2.** FTIR spectra of DHPDS-a system (a), focussed in to show band peaks (b).

without further purification treatment to avoid any uncontrolled oligo or polymerisation.

Fig. 1(b) shows the $^{13}$C NMR spectrum of DHPDS-a in DMSO-$d_6$. The peak assignments at 159.0 ppm (C-6 and C-6′), 155 ppm (C-11 and C-11′), 147.0 ppm (C-9 and C-9′), 135.0 ppm (C-7 and C-7′), 132.0–117.0 ppm (C-8 and C-8′, C-10 and C-10′, C-12 to C-16 and C-12′ to C-16′), 79.5 ppm (C-2 and C-2′) and 49.0 ppm (C-4 and C-4′) are consistent with the molecular structure of the monomer shown in Scheme 1.

FTIR analysis shown in Fig. 2 confirmed the aromatic ring stretches of C═C bonds of primary amine and benzoxazine, observed at 1599 cm$^{-1}$ and 1571 cm$^{-1}$, respectively. The peaks at 1495 cm$^{-1}$ and 1479 cm$^{-1}$ are assigned to C—C stretching vibrations of the disubstituted aromatic ring of the amine and substituted aromatic ring of the benzoxazine ring, respectively. $CH_2$ wagging of oxazine is observed at 1320 cm$^{-1}$. C–O–C asymmetric and symmetric stretches of the oxazine ring are observed at 1230 cm$^{-1}$ and 1082 cm$^{-1}$, respectively, whilst the oxazine ring C–N–C stretch is observed at 1121 cm$^{-1}$. The oxazine ring mode and out-of-plane bending vibration of C—H bond of the benzene ring attached to oxazine is observed at 934 cm$^{-1}$, thus confirming successful synthesis of the benzoxazine monomer. The bands from 871 cm$^{-1}$ to 755 cm$^{-1}$ are assigned to aromatic C—H bending vibrations. The ring-opening polymerisation of DHPDS-a is confirmed by the disappearance of oxazine ring-related spectral bands at 1230 cm$^{-1}$ and 934 cm$^{-1}$ in the FTIR spectrum of the polymer, which appears red in colour, different from the monomer, physically hard and chemically insoluble. This disappearance of significant peaks can be visualised in Fig. 2(b) which focuses in on the relevant region of the spectrum.

### 3.2. Thermo-mechanical characterisation

The 10°C min$^{-1}$ dynamic DSC thermograms of DHPDS-a and

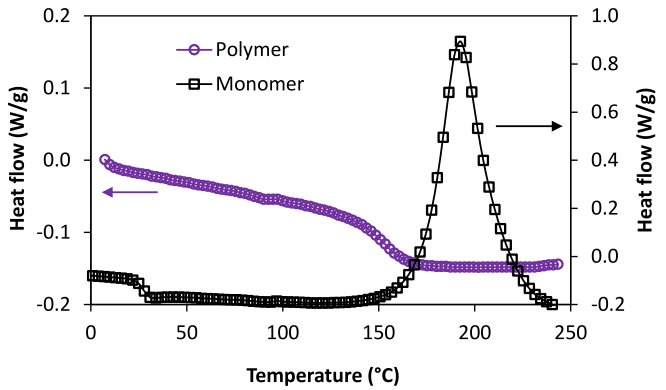


**Fig. 3.** DSC thermograms of DHPDS-a and polyDHPDS-a showing monomer $T_g$ of 27°C, cure exotherm and polymer $T_g$ of 155°C.

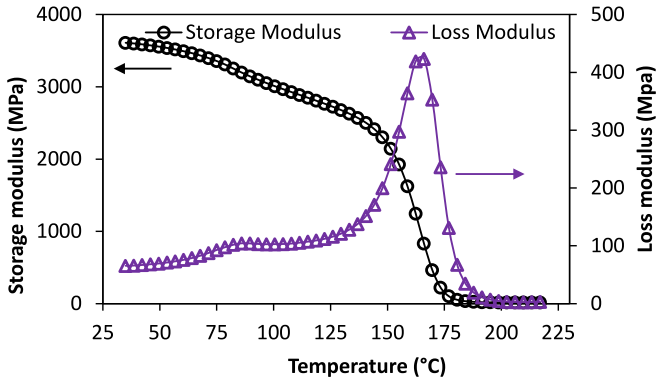


**Fig. 4.** DMA scan of polyDHPDS-a showing storage modulus and loss modulus.

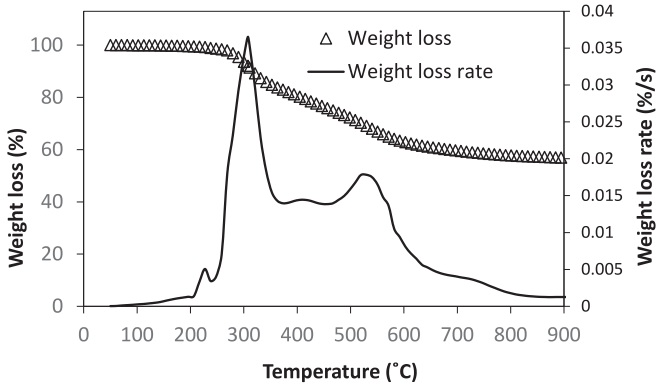


**Fig. 5.** TGA curves of polyDHPDS-an under 10°C $min^{-1}$ heating rate showing weight loss and rate of weight loss.

polyDHPDS-a are shown in Fig. 3, indicating a monomer $T_g$ of 25°C, polymerisation onset at 160°C, nearly symmetrical cure exotherm due to ring-opening polymerisation of benzoxazine with a single peak at 192°C, and $T_g$ of 155°C for the cured polymer. The measured heat of reaction determined using a sigmoidal baseline for integration of the heat flow signal is 206 J $g^{-1}$.

Fig. 4 illustrates the results of DMA testing. PolyDHPDS-a has a storage modulus of 3.6 GPa in the glassy state, with β-relaxation at 83°C, due to localised segmental motion within the polymer chain. The $T_g$ of polyDHPDS-a determined by the inflection in storage modulus is 164°C, a value that meets the requirements for $T_g$ range of high performance aerospace systems. This is comparable to the $T_g$ of 155°C determined by DSC, with the difference between the two values attributed to

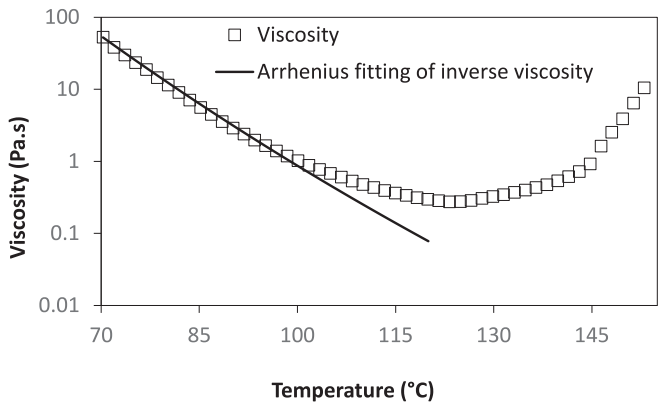


**Fig. 6.** Viscosity evolution in DHPDS-an under dynamic flow rheology and Arrhenius fitting of inverse viscosity at low temperature.

differences in the inherent frequency of the measurement and type of excitation, as well as in greater thermal lag in DMA due to its larger sample size. At the completion of α-relaxation, polyDHPDS-a has a plateau storage modulus of 14.9 MPa, measured at 206°C. The crosslinking density of the vitrimer determined using Eq. (2) is 1213 mol $m^{-3}$, which is expected for a polybenzoxazine that has a $T_g$ in the order of 155–164°C. This result can be compared with polybenzoxazines featuring crosslinking densities of 2900 and 12,760 mol $m^{-3}$, with $T_g$ values of 190–210°C and 300°C, respectively [30] and a benzoxazine vitrimer with a low crosslinking density of 208.4 mol $m^{-3}$ and a low $T_g$ of 40°C [19].

The results of thermogravimetric analysis of polyDHPDS-a reported in Fig. 5 show a 5% weight loss temperature of 293°C, indicating a greater thermal stability compared to a similar polybenzoxazine vitrimer which has a value of 252°C [19] and a sulphur-containing benzoxazine with lower thermal stability compared to its counterpart without sulphur [31]. As evident from the TGA curves, there is minimum weight loss up to 225°C, attributed to volatiles and trace impurities from benzoxazine precursors. A drop in weight from around 250°C, accompanied by a large peak in the weight loss rate curve at 308°C indicates decomposition of the material. PolyDHPDS-a exhibits a high char residue of 57.4% at 850°C, which, according to Eq. (1), corresponds to an estimated *LOI* of 40.5%. Whilst Eq. (1) is not accurate in determining *LOI*, it is often used to estimate its approximate value. Thus, the *LOI* of 40.5% is approximate. Materials with *LOI* between 21 and 30% are generally considered flame-retardant [32–36], whilst those with *LOI* above 40% are considered non-combustible [36]. The best fire-retardant polybenzoxazine in the literature has an *LOI* of 45.9% based on char yield measured at 800°C [37], with the greatest majority of benzoxazine formulations having values below the level exhibited by polyDHPDS-a [37]. The high *LOI* of polyDHPDS-a is attributed to the presence of many aromatic groups and the Mannich base bridge –$CH_2$–N(Phe)–$CH_2$– in the polymer structure as shown in Scheme 1. Whilst thermally less stable compared to BA-a with C—C bonds [38], DHPDS-a exhibits higher char yield than BA-a, due to the ability of S—S bonds to promote sulphur-rich residues and enhance aromatic stabilisation during pyrolysis, leading to increased char formation [31].

### 3.3. Rheology

The rheological behaviour of a monomer under processing conditions is crucial to its application in polymer composites manufacturing and governs the choice of manufacturing route, such as liquid moulding, prepreg or resin filming. Fig. 6 illustrates the rheological characteristics of DHPDS-a, depicting its viscosity evolution as a function of temperature at 2°C $min^{-1}$. At low temperatures, up to about 100°C, the viscosity decreases exponentially due to an increase in mobility with increasing

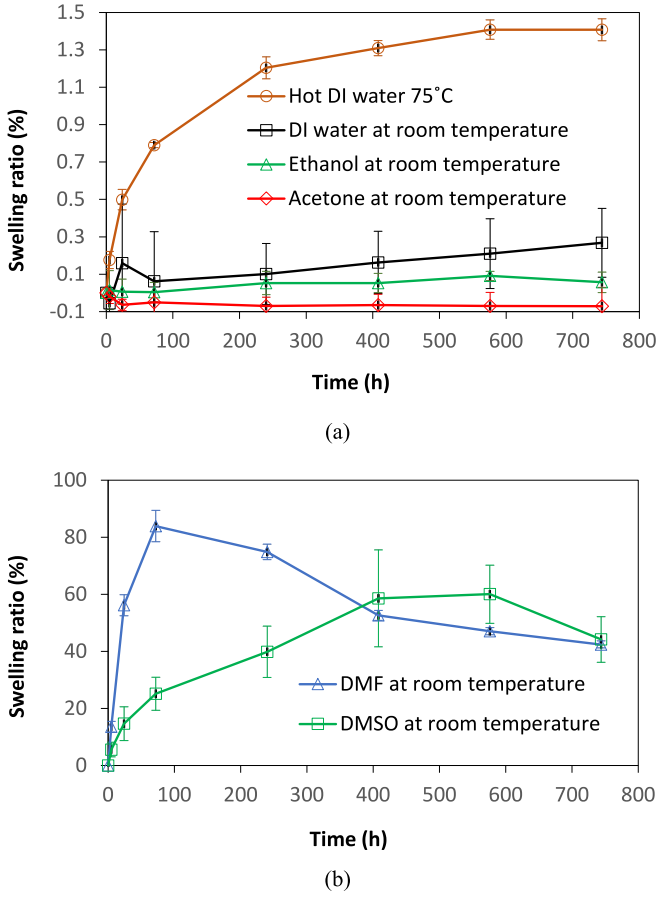


**Fig. 7.** Swelling behaviour of polyDHPDS-a in various solvents. Error bars correspond to one standard deviation.

**Table 1**
Swelling behaviour of polyDHPDS-a after 31 days immersion in various solvents.

| Solvent | Water | Water | Ethanol | Acetone | DMSO | DMF |
|---|---|---|---|---|---|---|
| T (°C) | 22 | 75 | 22 | 22 | 22 | 22 |
| *W* (%) | 0.27 | 1.41 | 0.06 | −0.07 | 44.17 | 42.42 |
| *M* (%) | 0.03 | 0.04 | 0.08 | 0.15 | 54.7 | 52.4 |

T Immersion temperature. *W* Swelling ratio. *M* Soluble fraction.

temperature. Over this temperature, the gradient of log viscosity versus temperature starts increasing as a result of the early stages of cross-linking. An Arrhenius-type fitting applied to the early stages of the experiment, visualises this effect. The temperature at which cross-linking is initialised is slightly over the synthesis temperature of 90°C. This implies that the synthesis at 90°C, could be accompanied by traces of pre-opened oxazine rings, as observed in the $^{1}$H NMR spectrum of Fig. 1(a), where bands attributed to the oligomers of benzoxazine are observed. Minimum viscosity at 2°C min$^{-1}$ of about 270 mPa s is observed at 125°C; beyond this temperature, crosslinking dominates the viscosity evolution, resulting in a fast increase with increasing temperature. The level of minimum viscosity is over the limit of around 100 mPa s which is commonly met in matrix systems appropriate for liquid moulding [39,40]. Therefore, the chemoviscosity of the material is suitable for manufacturing through filming or pre-impregnation.

### 3.4. Swelling behaviour

The swelling behaviour of polyDHPDS-a in different solvents is illustrated in Fig. 7 and summarised in Table 1. PolyDHPDS-a absorbs 0.27% water at room temperature (22 ± 2°C) after immersion for 31

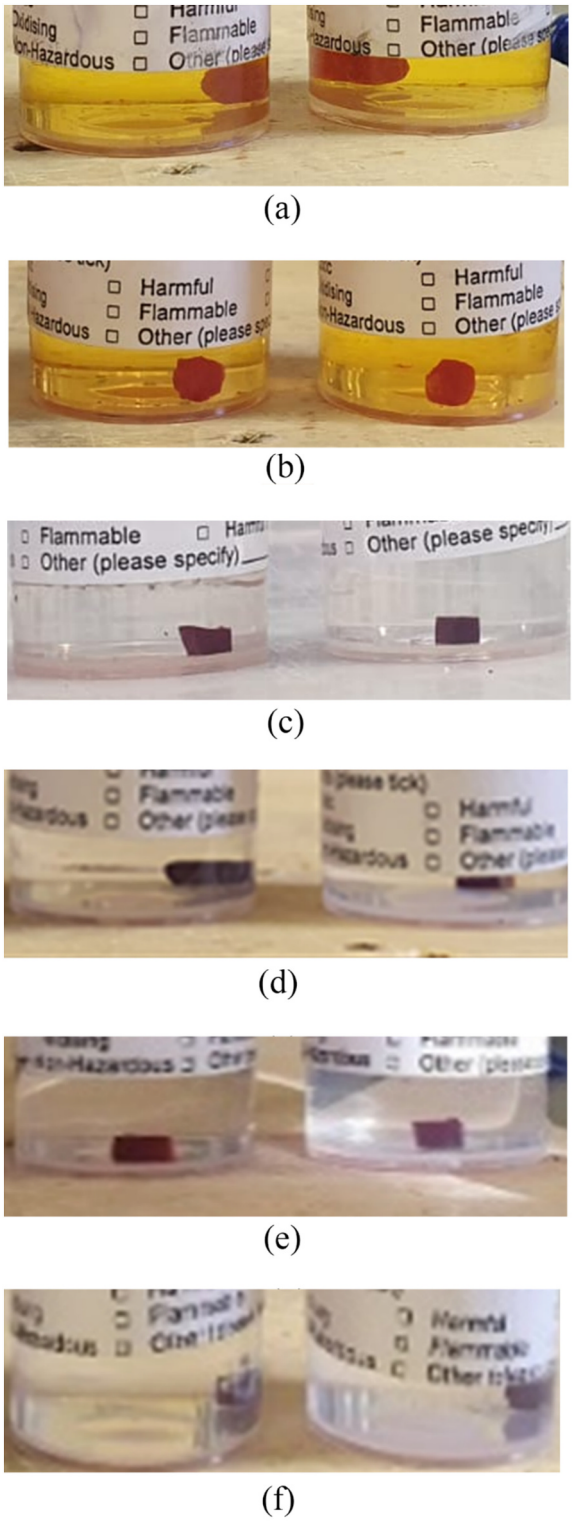


**Fig. 8.** Images of polyDHPDS-a in various solvents after 31 days of swelling tests: (a) yellow solution in DMF; (b) yellow solution in DMSO; (c) colourless solution in hot water; (d) colourless solution in ethanol; (e) colourless solution in acetone; (f) colourless solution in water at room temperature. (For interpretation of the references to colour in this figure legend, the reader is referred to the web version of this article.)

days. This is lower compared to characteristic values for high-temperature epoxy thermosets with $T_g$ similar or greater than that of polyDHPDS-a which show water uptake in the 1.2–2% range over equivalent periods [41]. After 31 days water immersion at an elevated temperature of 75°C, polyDHPDS-a swells by 1.4%. This is a better performance compared to high-$T_g$ epoxy resins, which undergo swelling in the 1.2–2.8% range in water at elevated temperatures in similar or less severe conditions [42,43]. The superior water absorption resistance of polyDHPDS-a compared to high-$T_g$ epoxies is attributed to lower polarity, compared to epoxies, of aromatic rings present in benzoxazines which increase hydrophobicity, in addition to the intramolecular N – $CH_2$ – N linkages in the network which enhance hydrolytic stability [44]. The moisture resistance of polyDHPDS-a is also comparable to that of high-$T_g$ polybenzoxazine composites which undergo swelling of about 1.7–2% after immersion in water at 80°C [45,46]. The soluble fractions of polyDHPDS-a in DI water after soaking for 31 days at room temperature and at 75°C are 0.03% and 0.04%, respectively.

PolyDHPDS-a is resistant to both ethanol and acetone, exhibiting uptakes of 0.06% and – 0.07%, respectively in these solvents after soaking for 31 days. The negative value may be attributed to a combined effect of: (i) solute dissolution dominating over solvent uptake, as more solute particles go into solution than solvent is absorbed by the solute, (ii) high volatility of acetone, such that any absorbed acetone could quickly evaporate during weighing, resulting in a weight loss rather than a gain. The swelling behaviour of polyDHPDS-a in ethanol and acetone is similar, or better, compared to epoxy thermosets which are reported to exhibit swelling ratio ranging from 0.3 to 12% at 35°C [47]. After 31 days of soaking at room temperature, polyDHPDS-a has dissolved fractions of 0.15% and 0.08% in acetone and ethanol, respectively.

Fig. 8 shows samples of polyDHPDS-a in solvents after 31 days of immersion. In the case of room temperature DI water, ethanol, acetone and water at 75°C, the solvents remain colourless which indicates negligible to low dissolution. Samples in DMF and DMSO, which substantially swell and dissolve, change the colour of the solvents after the 31 days immersion period from colourless to brown. The change in colour indicates gradual dissolution of the polymer in these two solvents due to similarity of polarity [48].

The swelling in DMF initially increases sharply due to strong dipole-dipole interactions between the solvent and the resin. After 3 days of soaking at room temperature, polyDHPDS-a is saturated by DMF with a swelling ratio of 83.9% as seen in Fig. 7(b), and the material begins to lose weight due to dissolution of the material by the solvent. At this point, mass uptake in DMSO continues increasing with swelling of 25.2%. It takes about 17 days for DMSO to saturate polyDHPDS-a, plateauing at a swelling ratio of about 60% after 21 days before weight loss due to dissolution. The nitrogen and oxygen atoms in oxazine ring of benzoxazine have lone pairs of electrons which create dipoles, giving benzoxazine polar characteristics. Additionally, the -OH group in benzoxazine, resulting from ring-opening polymerisation, enhances its polarity. Therefore, DMF and DMSO, being strongly aprotic polar solvents, are excellent swelling agents for polybenzoxazines, in much the same way they do to other polar resins, such as epoxies [49,50]. This has been demonstrated with a carbon fibre epoxy composite with swelling ratios of 83.6%, and 85.0% after 1 h immersion at 120°C in DMF and DMSO, respectively [51].

After 31 days immersion, polyDHPDS-a shows dissolved fractions of 54.7% and 52.4% in DMSO and DMF, respectively, in line with the results of previously reported vitrimers with very high dissolved fractions within 48 h [19,52]. This level of dissolved fraction is expected, given the polymer has a low crosslinking density (1213 mol $m^{-3}$) compared to conventional epoxies.

### 3.5. Stress relaxation

The isothermal stress relaxation behaviour of polyDHPDS-a is shown in Fig. 9(a) and the normalised stress relaxation data in Fig. 9(b). The relaxation follows an exponential decay with the relaxation time corresponding to the time required for the modulus to drop by 1/e of its plateau value. From these results, the relaxation time at 175°C is 16 s, whilst at 195°C, the relaxation time is 4 s, which suggest good healing behaviour at these temperatures. The relaxation time as a function of inverse absolute temperature is illustrated in Fig. 10 alongside the corresponding Arrhenius dependence fit. The exponential fit follows the experimental data closely with a coefficient of determination of 0.998. The activation energy of the bond exchange is 127 kJ $mol^{-1}$.

The complex rubbery modulus of polyDHPDS-a from dynamic single frequency temperature ramp DMA results shown in Fig. 4 (14.9 MPa)

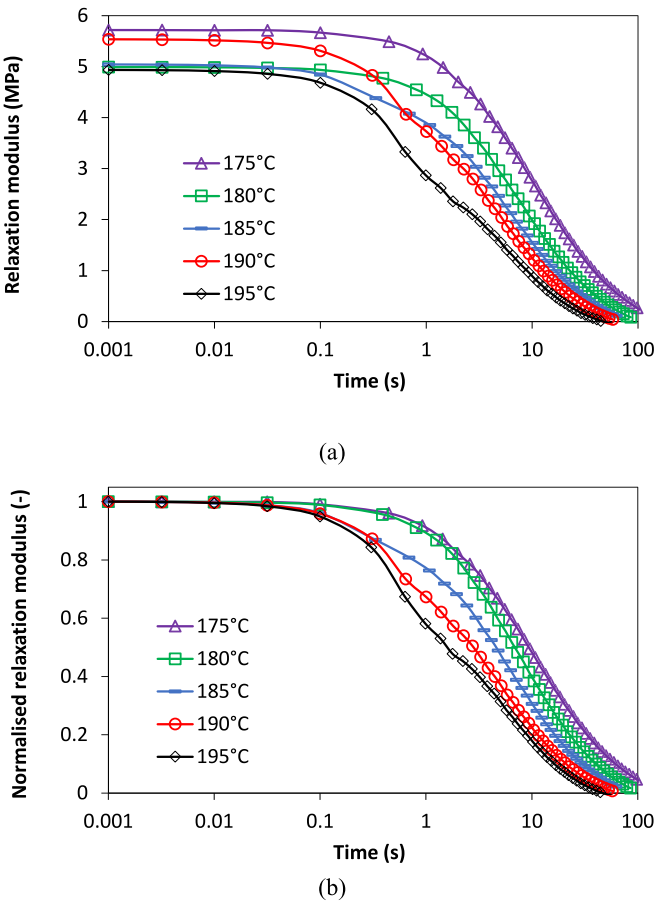


**Fig. 9.** Stress relaxation curves of polyDHPDS-a. (a) Relaxation modulus versus time (b) Normalised stress relaxation curves.

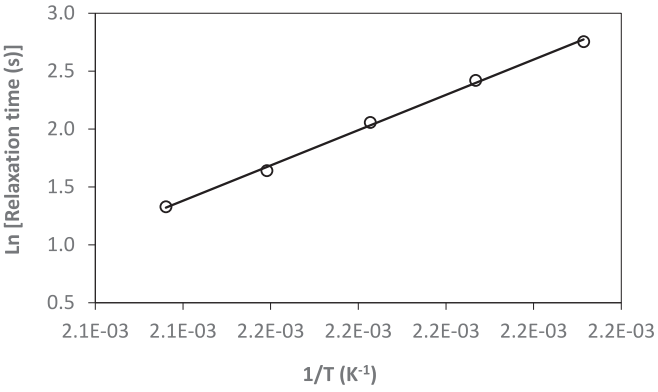


**Fig. 10.** Arrhenius temperature dependence of relaxation time

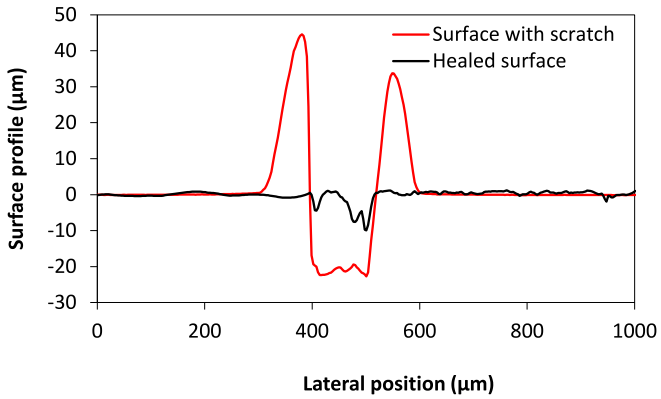


**Fig. 11.** Surface profiles of unhealed and healed polyDHPDS-a specimen.

**Table 2**
Surface areas affected by scratching before and after healing of polyDHPDS-a.

| | Unhealed specimen | Healed specimen | % Recovery |
|---|---|---|---|
| Lips ($\mu m^2$) | 2694 | 213 | 92.1 |
| Valley ($\mu m^2$) | 2542 | 435 | 82.9 |
| Overall ($\mu m^2$) | 5236 | 648 | 87.6 |

can be used to calculate the topological transition temperature ($T_v$), taken as the temperature at which the viscosity becomes $10^{12}$ Pa s, corresponding to a relaxation time of 201,800 s. $T_v$ is determined as the temperature at which the Arrhenius dependence reported in Fig. 10 reaches this value and is equal to 78°C. The $T_v$ and activation energy of polyDHPDS-a are similar to those of a disulphide bond-enabled epoxy vitrimer which has a $T_v$ of 75°C and dynamic bond exchange activation energy of 126 kJ $mol^{-1}$ [4,53] as well as another set of disulphide bond-based epoxy vitrimers having topological transition temperatures of 85.7°C and 141.1°C and activation energies of 128.9 kJ $mol^{-1}$ and 165.6 kJ $mol^{-1}$, respectively [5]. Typical of metathesis vitrimers, the $T_v$ of polyDHPDS-a is below its $T_g$ of 155°C. Therefore, bond exchange is frozen in the material when the temperature is below the $T_g$. Upon reaching the $T_g$, fast dynamic bond exchange is triggered, enabling reprocessing to be carried out.

### 3.6. Self-healing behaviour

The surface profiles of scratched polyDHPDS-a measured before and after healing at 190°C for 15 min are shown in Fig. 11. The scratch has an approximate width of about 100 µm and a depth of about 25 µm, with lips of a height of 30–40 µm and a base of about 70 µm. The approximate cross-sectional areas of the scratch are reported in Table 2. The scratch is almost fully recovered after the healing. The overall recovery of the scratch is about 88%, indicating very effective healing, within timelines and temperatures fully compatible with composite manufacturing strategies. The prospect of DHPDS-a as a high-temperature moisture-resistant composite matrix with char yield up to 57%, reprocessable at 190°C is an attractive option for the future of aerospace industry.

## 4. Conclusions

The benzoxazine system reported in this work (polyDHPDS-a) is the first high-temperature benzoxazine vitrimer synthesised via the cost-effective one-pot solventless method. It features a $T_g$ of 155°C, a glass modulus of 3.6 GPa, potential for fire retardancy as indicated by an *LOI* of 40.5%, relatively high thermal stability with $T_{d5\%}$ of 293°C, high environmental resistance, demonstrated by equilibrium water absorption of only 1.4% around its topology freezing transition temperature, and solvent resistance. PolyDHPDS-a has a $T_v$ of 78°C, which is below its $T_g$, resulting in fast reversible bond exchange which occurs with the onset of $T_g$. Therefore, it is anticipated that fibre composites with polyDHPDS-a matrix would be reprocessable at 190°C, due to the fast stress relaxation at this temperature enabled by reversible disulphide bond exchange. This would be confirmed in another study. The properties of polyDHPDS-a reported in this study establish it as a candidate for a broad spectrum of functionalities, such as self-healing, high-temperature, fire retardant, environmentally resistant application, corresponding well to the future requirements for matrix system of sustainable composites for the aerospace, marine and energy sectors.

## CRediT authorship contribution statement

**Festus Ifeanyi Anagwu:** Writing – review & editing, Writing – original draft, Visualization, Validation, Software, Resources, Project administration, Methodology, Investigation, Funding acquisition, Formal analysis, Data curation, Conceptualization. **Eleftheria Dossi:** Writing – review & editing, Visualization, Validation, Methodology, Investigation, Formal analysis, Data curation. **Alexandros A. Skordos:** Writing – review & editing, Visualization, Validation, Supervision, Software, Resources, Project administration, Formal analysis, Data curation, Conceptualization.

## Declaration of competing interest

The authors declare that they have no known competing financial interests or personal relationships that could have appeared to influence the work reported in this paper.

## Acknowledgements

This research was supported by the Tertiary Education Trust Fund, Nigeria, through the overseas scholarship award grant reference TETF/ES/POLY/IMO STATE/TSAS/2019/VOL.I.

## Data availability

Dataset underlying this study and its description can be accessed through the Figshare repository at doi:https://doi.org/10.6084/m9.figshare.26196461

## References

[1] D. Montarnal, M. Capelot, F. Tournilhac, L. Leibler, Silica-like malleable materials from permanent organic networks, Science 334 (2011) 965–968, https://doi.org/10.1126/science.1212648.
[2] A. Ruiz de Luzuriaga, G. Solera, I. Azcarate-Ascasua, V. Boucher, H.J. Grande, A. Rekondo, Chemical control of the aromatic disulphide exchange kinetics for tailor-made epoxy vitrimers, Polymer 239 (2022) 124457, https://doi.org/10.1016/j.polymer.2021.124457.
[3] A. Ruiz de Luzuriaga, N. Markaide, A.M. Salaberria, I. Azcune, A. Rekondo, H. J. Grande, Aero grade epoxy vitrimer towards commercialization, Polymers 14 (2022) 3180, https://doi.org/10.3390/polym14153180.
[4] A. Ruiz De Luzuriaga, R. Martin, N. Markaide, A. Rekondo, G. Cabañero, J. Rodríguez, I. Odriozola, Epoxy resin with exchangeable disulphide crosslinks to obtain reprocessable, repairable and recyclable fiber-reinforced thermoset composites, Mater. Horiz. 3 (2016) 241–247, https://doi.org/10.1039/c6mh00029k.
[5] C. Luo, W. Wang, W. Yang, X. Liu, J. Lin, L. Zhang, S. He, High-strength and multi-recyclable epoxy vitrimer containing dual-dynamic covalent bonds based on the disulphide and imine bond metathesis, ACS Sustain. Chem. Eng. 11 (2023) 14591–14600, https://doi.org/10.1021/acssuschemeng.3c04345.
[6] X. Wang, S. Zhang, Y. He, W. Guo, Z. Lu, Reprocessable polybenzoxazine thermosets with high $T_g$s and mechanical strength retentions using boronic ester bonds as crosslinkages, Polymers 14 (2022) 2234, https://doi.org/10.3390/polym14112234.
[7] A. Adjaoud, L. Puchot, C.E. Federico, R. Das, P. Verge, Lignin-based benzoxazines: a tunable key-precursor for the design of hydrophobic coatings, fire resistant materials and catalyst-free vitrimers, Chem. Eng. J. 453 (2023) 139895, https://doi.org/10.1016/j.cej.2022.139895.
[8] A. Adjaoud, L. Puchot, P. Verge, High – $T_g$ and degradable isosorbide-based polybenzoxazine vitrimer, ACS Sustain. Chem. Eng. 10 (2022) 594–602, https://doi.org/10.1021/acssuschemeng.1c07093.

[9] A. Adjaoud, A. Trejo-Machin, L. Puchot, P. Verge, Polybenzoxazines: a sustainable platform for the design of fast responsive and catalyst-free vitrimers based on transesterification exchanges, Polym. Chem. 12 (2021) 3276–3289, https://doi.org/10.1039/d1py00324k.

[10] A. Adjaoud, B. Marcolini, R. Dieden, L. Puchot, P. Verge, Deciphering the self-catalytic mechanisms of polymerization and transesterification in polybenzoxazine vitrimers, J. Am. Chem. Soc. 146 (2024) 13367–13376, https://doi.org/10.1021/jacs.4c02153.

[11] C. Bo, Y. Sha, F. Song, M. Zhang, L. Hu, P. Jia, Y. Zhou, Renewable benzoxazine-based thermosets from cashew nut: investigating the self-healing, shape memory, recyclability and antibacterial activity, J. Clean. Prod. 341 (2022) 130898, https://doi.org/10.1016/j.jclepro.2022.130898.

[12] Z. Wen, L. Bonnaud, P. Dubois, J.M. Raquez, Catalyst-free reprocessable crosslinked biobased polybenzoxazine-polyurethane based on dynamic carbamate chemistry, J. Appl. Polym. Sci. 139 (2022) 1–8, https://doi.org/10.1002/app.52120.

[13] S. Gulyuz, Y. Yagci, B. Kiskan, Exploiting the reversible covalent bonding of boronic acids for self-healing/recycling of main-chain polybenzoxazines, Polym. Chem. 13 (2022) 3631–3638, https://doi.org/10.1039/d2py00068g.

[14] L. Pursche, A. Wolf, T. Urbaniak, K. Koschek, Benzoxazine/amine-based polymer networks featuring stress-relaxation and reprocessability, Front. Soft Matter 3 (2023), https://doi.org/10.3389/frsfm.2023.1197868.

[15] L.J. Hamernik, W. Guzman, J.S. Wiggins, Solvent-free preparation of imine vitrimers: leveraging benzoxazine crosslinking for melt processability and tunable mechanical performance, J. Mater. Chem. A 11 (2023) 20568–20582, https://doi.org/10.1039/d3ta04351g.

[16] H. Ishida, Overview and historical background of polybenzoxazine research, in: H. Ishida, T. Agag (Eds.), Handbook of Benzoxazine Resins, 1st ed, Elsevier Ltd, Amsterdam, 2011, pp. 3–81, https://doi.org/10.1016/b978-0-444-53790-4.00046-1.

[17] Z. Zhu, S. West, H. Chen, G.-H. Lai, S. Uenuma, K. Ito, M. Kotaki, H.-J. Sue, Mechanically interlocked vitrimer based on polybenzoxazine and polyrotaxane, ACS Appl. Polym. Mater. 5 (2023) 3971–3978, https://doi.org/10.1021/acsapm.3c00196.

[18] A. Ruiz De Luzuriaga, R. Martin, N. Markaide, A. Rekondo, G. Cabañero, J. Rodríguez, I. Odriozola, Epoxy resin with exchangeable disulphide crosslinks to obtain reprocessable, repairable and recyclable fiber-reinforced thermoset composites, Mater. Horiz. 3 (2016) 241–247, https://doi.org/10.1039/c6mh00029k.

[19] A. Trejo-Machin, L. Puchot, P. Verge, A cardanol-based polybenzoxazine vitrimer: recycling, reshaping and reversible adhesion, Polym. Chem. 11 (2020) 7026–7034, https://doi.org/10.1039/d0py01239d.

[20] A. Adjaoud, L. Puchot, P. Verge, Polybenzoxazine-based covalent adaptable networks: a mini-review, Polymer 287 (2023) 126426, https://doi.org/10.1016/j.polymer.2023.126426.

[21] A.W. Kawaguchi, A. Sudo, T. Endo, Synthesis of highly polymerizable 1,3-benzoxazine assisted by phenyl thio ether and hydroxyl moieties, J. Polym. Sci. Part A: Polym. Chem. 50 (2012) 1457–1461, https://doi.org/10.1002/pola.25923.

[22] A.W. Kawaguchi, A. Sudo, T. Endo, Thiol-functionalized 1,3-benzoxazine: preparation and its use as a precursor for highly polymerizable benzoxazine monomers bearing sulphide moiety, J. Polym. Sci., Part A: Polym. Chem. 52 (2014) 1448–1457, https://doi.org/10.1002/pola.27131.

[23] T. Endo, A. Sudo, Molecular designs of benzoxazines with enhanced reactivity based on utilization of neighboring-group participation and introduction of thioether moiety, in: H. Ishida, P. Froimowicz (Eds.), Advanced and Emerging Polybenzoxazine Science and Technology, Elsevier, 2017, pp. 23–33, https://doi.org/10.1016/B978-0-12-804170-3.00003-2.

[24] D.W. van Krevelen, Some basic aspects of flame resistance of polymeric materials, Polymer 16 (1975) 615–620, https://doi.org/10.1016/0032-3861(75)90157-3.

[25] Bis(4-Hydroxyphenyl) Disulphide Safety Data Sheet, Ambeed, Inc, USA, 2023. https://file.ambeed.com/static/upload/prosds/am/184/SDS-A183502.pdf (accessed October 23, 2023).

[26] Aniline Safety Data Sheet, ThermoFisher Scientific, 2020. https://assets.thermofisher.com/DirectWebViewer/private/document.aspx?prd=ACR15819~~PDF~~MTR~~CGV4~~EN~~2022-04-02%2018:09:08~~Aniline~~ (accessed 23 October 2023).

[27] Paraformaldehyde Safety Data Sheet, Sigma-Aldrich, 2019. https://www.sigmaaldrich.com/GB/en/product/sial/p6148 (accessed 4 March 2021).

[28] H. Ishida, Process for Preparation of Benzoxazine Compounds in Solventless Systems, 5543516. https://patentimages.storage.googleapis.com/f0/58/d7/88aa918889bd08/US5543516.pdf, 1996.

[29] F.I. Anagwu, E. Dossi, A.A. Skordos, Dataset supporting High-glass transition catalyst-free polybenzoxazine vitrimer through one-pot solventless method [dataset], Figshare Repos. (2024), https://doi.org/10.6084/m9.figshare.26196461.

[30] K.S. Santhosh Kumar, C.P. Reghunadhan Nair, T.S. Radhakrishnan, K.N. Ninan, Bis allyl benzoxazine: synthesis, polymerisation and polymer properties, Eur. Polym. J. 43 (2007) 2504–2514, https://doi.org/10.1016/j.eurpolymj.2007.03.028.

[31] M. Arslan, B. Kiskan, Y. Yagci, Combining elemental sulphur with polybenzoxazines via inverse vulcanization, Macromolecules 49 (2016) 767–773, https://doi.org/10.1021/acs.macromol.5b02791.

[32] M.I. Nelson, A dynamical systems model of the limiting oxygen index test: II. Retardancy due to char formation and addition of inert fillers, Combust. Theory Model. 5 (2001) 59–83, https://doi.org/10.1088/1364-7830/5/1/304.

[33] S. Basak, Kartick.K. Samanta, S. Saxena, S.K. Chattopadhyay, R. Narkar, R. Mahangade, G.B. Hadge, Flame resistant cellulosic substrate using banana pseudostem sap, Pol. J. Chem. Technol. 17 (2015) 123–133. https://doi.org/10.1515/pjct-2015-0018.

[34] A.R. Horrocks, M. Tune, L. Cegielka, The burning behaviour of textiles and its assessment by oxygen-index methods, Text. Prog. 18 (1988) 1–186, https://doi.org/10.1080/00405168908689004.

[35] C.P. Fenimore, Candle-type test for flammability of polymers, in: Lewin Menachem, S.M. Atlas, E.M. Pearce (Eds.), Flame-Retardant Polymeric Materials, Springer US, Boston, MA, 1975, pp. 371–397, https://doi.org/10.1007/978-1-4684-2148-4_9.

[36] R.E. Lyon, R.N. Walters, S.I. Stoliarov, Thermal analysis of flammability, J. Therm. Anal. Calorim. 89 (2007) 441–448, https://doi.org/10.1007/s10973-006-8257-z.

[37] I. Machado, C. Shaer, K. Hurdle, V. Calado, H. Ishida, Towards the development of green flame retardancy by polybenzoxazines, Prog. Polym. Sci. 121 (2021) 101435, https://doi.org/10.1016/j.progpolymsci.2021.101435.

[38] A.B. Rajput, N.N. Ghosh, Preparation and characterization of novel polybenzoxazine–polyester resin blends, Int. J. Polym. Mater. 60 (2010) 27–39, https://doi.org/10.1080/00914037.2010.504153.

[39] Solvay CYCOM 890 RTM resin safety data sheet. https://www.syensqo.com/en/downloadDocument?fileId=Tvs6udByG6GY9YWs6j&fileName=CYCOM%20890%20RTM_CM_EN&base=FAST, 2017 (accessed 14 November 2024).

[40] HexFlow RTM6/RTM6–2 Product Data Sheet, 2023. https://www.hexcel.com/user_area/content_media/raw/rtm6_rtm62_hexflow_datasheet(1).pdf (accessed 6 August 2023).

[41] A.F. Abdelkader, J.R. White, Water absorption in epoxy resins: the effects of the crosslinking agent and curing temperature, J. Appl. Polym. Sci. 98 (2005) 2544–2549, https://doi.org/10.1002/app.22400.

[42] K. Shetty, R. Bojja, S. Srihari, Effect of hygrothermal aging on the mechanical properties of IMA/M21E aircraft-grade CFRP composite, Adv. Compos. Lett. 29 (2020) 2633366X2092652, https://doi.org/10.1177/2633366X20926520.

[43] A. Simar, M. Gigliotti, J.C. Grandidier, I. Ammar-Khodja, Evidence of thermo-oxidation phenomena occurring during hygrothermal aging of thermosetting resins for RTM composite applications, Compos. Part A Appl. Sci. Manuf. 66 (2014) 175–182, https://doi.org/10.1016/j.compositesa.2014.07.007.

[44] S. Gulyuz, B. Kiskan, Combination of polyethylenimine and vanillin-based benzoxazine as a straightforward self-healable system with excellent film-forming ability, Macromolecules 57 (2024) 2078–2089, https://doi.org/10.1021/acs.macromol.4c00005.

[45] N.H. Nash, D. Ray, T.M. Young, W.F. Stanley, The influence of hydrothermal conditioning on the mode-I, thermal and flexural properties of carbon/Benzoxazine composites with a thermoplastic toughening interlayer, Compos. Part A Appl. Sci. Manuf. 76 (2015) 135–144, https://doi.org/10.1016/j.compositesa.2015.04.023.

[46] A.J. Comer, D. Ray, G. Clancy, W.O. Obande, I. Rosca, P.T. McGrail, W.F. Stanley, Hydrothermal in-plane-shear strength of carbon fibre/benzoxazine laminates manufactured out-of-autoclave by liquid-resin-infusion, Compos. Struct. 213 (2019) 261–270, https://doi.org/10.1016/j.compstruct.2019.01.069.

[47] F. Wolff, C.-G. Kim, Swelling behaviour of epoxy resins in various solvent systems, in: 21st Int. Conf. Compos. Mater., Xi'an, China, 2017. http://smartech.kaist.ac.kr/ (accessed February 19, 2023).

[48] P. Zhu, Y.Z. Yang, Y. Chen, G.R. Qian, Q. Liu, Influence factors of determining optimal organic solvents for swelling cured brominated epoxy resins to delaminate waste printed circuit boards, J. Mater. Cycles Waste Manag. 20 (2018) 245–253, https://doi.org/10.1007/s10163-016-0574-0.

[49] M. Tatariants, S. Yousef, G. Denafas, R. Bendikiene, Separation and purification of metal and fiberglass extracted from waste printed circuit boards using milling and dissolution techniques, environ, Prog. Sustain Energy 37 (2018) 2082–2092, https://doi.org/10.1002/ep.12899.

[50] H.R. Verma, K.K. Singh, T.R. Mankhand, Dissolution and separation of brominated epoxy resin of waste printed circuit boards by using di-methyl formamide, J. Clean. Prod. 139 (2016) 586–596, https://doi.org/10.1016/j.jclepro.2016.08.084.

[51] Z. Li, M. Xing, L. Zhao, Z. Li, Y. Wang, Recovery of carbon fiber-reinforced polymer waste using dimethylacetamide base on the resin swelling principle, Front. Chem. 10 (2022) 1050827, https://doi.org/10.3389/fchem.2022.1050827.

[52] S. Dhers, G. Vantomme, L. Avérous, A fully bio-based polyimine vitrimer derived from fructose, Green Chem. 21 (2019) 1596–1601, https://doi.org/10.1039/c9gc00540d.

[53] A. Ruiz De Luzuriaga, R. Martin, N. Markaide, A. Rekondo, G. Cabañero, J. Rodríguez, I. Odriozola, Correction: epoxy resin with exchangeable disulphide crosslinks to obtain reprocessable, repairable and recyclable fiber-reinforced thermoset composites, Mater. Horiz. 7 (2020) 2460–2461, https://doi.org/10.1039/d0mh90047h.

# High glass transition catalyst-free polybenzoxazine vitrimer through one-pot solventless method

Anagwu, Festus Ifeanyi

2025-04



Anagwu FI, Dossi E, Skordos AA. (2025) High glass transition catalyst-free polybenzoxazine vitrimer through one-pot solventless method. Reactive and Functional Polymers, Volume 209, April 2025, Article number 106186

https://doi.org/10.1016/j.reactfunctpolym.2025.106186